

TUM-HEP-842/12
TTK-12-23
ITP-UU-12/21
SPIN-12/19
FR-PHENO-2012-010
SFB/CPP-12-34
1206.2454 [hep-ph]
July 27, 2012

Inclusive top-pair production phenomenology with TOPIX

M. BENEKE^{a,b}, P. FALGARI^c, S. KLEIN^b, J. PICLUM^{a,b}, C. SCHWINN^d,
M. UBIALI^b, F. YAN^b

^a*Physik Department T31,
James-Franck-Straße, Technische Universität München,
D-85748 Garching, Germany*

^b*Institut für Theoretische Teilchenphysik und Kosmologie,
RWTH Aachen University, D-52056 Aachen, Germany*

^c*Institute for Theoretical Physics and Spinoza Institute,
Utrecht University, 3508 TD Utrecht, The Netherlands*

^d*Albert-Ludwigs Universität Freiburg, Physikalisches Institut,
D-79104 Freiburg, Germany*

Abstract

We discuss various aspects of inclusive top-quark pair production based on TOP-IXS, a new, flexible program that computes the production cross section at the Tevatron and LHC at next-to-next-to-leading logarithmic accuracy in soft and Coulomb resummation, including bound-state effects and the complete next-to-next-to-leading order result in the $q\bar{q}$ channel, which has recently become available. We present the calculation of the top-pair cross section in pp collisions at 8 TeV centre-of-mass energy, as well as the cross sections for hypothetical heavy quarks in extensions of the standard model. The dependence on the parton distribution input is studied. Further we investigate the impact of LHC top cross section measurements at $\sqrt{s} = 7$ TeV on global fits of the gluon distribution using the NNPDF re-weighting method.

1 Introduction

The measurement of the inclusive top-quark pair production cross section is currently of great interest at the Large Hadron Collider (LHC). It provides constraints on models that explain the anomalous forward-backward asymmetry by new physics; measures the top-quark mass cleanly, though not very precisely; is sensitive to the gluon distribution in the proton in a momentum-fraction region that is not well constrained by other measurements; and it serves as a template for searches for unknown particles with missing transverse momentum. For all these reasons a precise cross section calculation is desirable, and, in fact, the top-quark pair production cross section is by now the most precisely predicted purely hadronic high-energy cross section.

In [1] some of us presented a calculation of the top-quark pair production cross section that included the threshold approximation to the next-to-next-to-leading-order (NNLO) partonic cross sections [2], the joint resummation of soft and Coulomb corrections to all orders with next-to-next-to-leading logarithmic (NNLL) accuracy, and bound-state effects due to Coulomb attraction. The calculation of [1] therefore constitutes the most complete implementation of the inclusive production cross section. With the present paper we release the first version of the user-friendly public program TOPIXS (“TOP-pair Inclusive X[*cross*] Section”), which incorporates the calculation of [1] and an important update as described below. The functionality of the program is described in the appendix of this paper. The program, together with a detailed manual, can be obtained from the URL

<http://users.ph.tum.de/t31software/topixs/>

which will be continuously updated. Other publicly available implementations beyond NLO exist [3–5] and agree at the few-percent level, but do not include soft-gluon resummation (HATHOR) and Coulomb resummation (HATHOR, top++) to all orders, while the program provided with [6] obtains the inclusive cross section from resummed or approximated differential distributions. Further approximate NNLO results have been obtained in [7, 8].

In the following sections of this work, we consider various topics extending our previous results [1], which are motivated by recent theoretical developments and the anticipated data of the 2012 LHC run:

- We include the (almost) exact NNLO $q\bar{q}$ partonic cross section, which has recently become available [9]. This decreases the cross section in $p\bar{p}$ collisions at the Tevatron by about 1%, together with its theoretical uncertainty, but has a negligible effect on pp collisions (LHC).
- We provide results for $\sqrt{s} = 8$ TeV, since meanwhile the LHC centre-of-mass energy has been increased to this value.
- In [1] we exclusively used the MSTW2008 parton distribution functions (PDFs) [10]. Here we compare the predictions for different PDF sets, since, given the accuracy of the partonic calculation, the PDF error is now the most important single theoretical

uncertainty. Results for different PDFs based on the program HATHOR [3] can also be found in [11].

- It is very likely that a perturbative sequential fourth generation will be excluded (or discovered) in the 2012 LHC run. Heavy vector-like fermions with Standard Model (SM) QCD interactions may exist in other models. We therefore present production cross sections for a hypothetical heavy “top” quark.
- The possibility to constrain the gluon distribution in the proton through the top production cross section has been mentioned in [12, 13]. With precise theoretical calculations and LHC data at $\sqrt{s} = 7$ TeV, this can now be investigated in practice. We quantify the impact of the existing data on global fits of the gluon distribution using the NNPDF re-weighting method presented in [14, 15], including the case when the jet data is left out from the “global” fit.

The reader interested in the theoretical framework of soft-gluon and Coulomb resummation is referred to [1] and [16, 17].

2 Updated cross-sections

2.1 Theoretical framework for NNLO+NNLL

The total partonic top-pair production cross section depends on the top-quark mass and the kinematic variable $\beta = \sqrt{1 - 4m_t^2/\hat{s}}$. In [1] singular terms as $\beta \rightarrow 0$ were summed to all orders at NNLL accuracy by representing the cross section in the form [17]

$$\hat{\sigma}_{pp'}^{\text{NNLL}}(\hat{s}, \mu) = \sum_{R=1,8} H_{pp'}^R(m_t, \mu) \int d\omega J_R(E - \frac{\omega}{2}) W^R(\omega, \mu), \quad (2.1)$$

where $E = \sqrt{\hat{s}} - 2m_t$ is the energy relative to the production threshold. The soft functions W_R sum logarithms of β from soft-gluon emission. The potential function J_R sums Coulomb-gluon exchange related to the attractive or repulsive Coulomb force in the colour-singlet and octet channels, respectively. Logarithms of β from non-relativistic physics are currently included at NNLO in J_R . The hard functions H_R account for the short-distance production process of the $t\bar{t}$ pair. The momentum-space approach to threshold resummation [18, 19] is employed, where renormalization-group equations evolve the hard functions from a hard scale μ_h to the factorization scale μ_f and the soft function from the soft scale $\mu_s \sim m_t\beta^2$ to μ_f . As default the values $\mu_h = 2m_t$, $\mu_f = m_t$ and a “running” soft scale $\mu_s = 2m_t \max[\beta^2, \beta_{\text{cut}}^2]$ is used. An alternative method with a fixed soft scale, and the determination of β_{cut} are discussed in detail in [1].

Since (2.1) is strictly valid only for small β , the expression is matched to the available fixed-order computations. In [1] the final results were based on the matching equation

$$\hat{\sigma}_{pp'/\text{matched},2}^{\text{NNLL}}(\hat{s}) = \left[\hat{\sigma}_{pp'}^{\text{NNLL}}(\hat{s}) - \hat{\sigma}_{pp'}^{\text{NNLL}(2)}(\hat{s}) \right] + \hat{\sigma}_{pp'}^{\text{NLO}}(\hat{s}) + \hat{\sigma}_{\text{app},pp'}^{\text{NNLO}}(\hat{s}), \quad (2.2)$$

where $\hat{\sigma}_{pp'}^{\text{NNLL}^{(2)}}(\hat{s})$ is (2.1) expanded to $\mathcal{O}(\alpha_s^2)$ relative to the Born cross section, and the last two terms represent the fixed-order NLO cross section plus the threshold approximation of the NNLO terms [2]. That is, the partonic cross section consisted of all known fixed-order terms with the $\mathcal{O}(\alpha_s^n)$ terms with $n > 2$ from the resummation formula (2.1) added.¹

This can now be improved. The full NNLO partonic cross section, not restricted to small β , has recently been computed [9] for the $q\bar{q}$ initial state, except for the partonic processes $q\bar{q} \rightarrow t\bar{t}q\bar{q}$ with same-flavour (anti-)quarks in the initial and final state, which are presumed to be small. The matching equation (2.2) is straightforwardly modified to include this important result by substituting

$$\hat{\sigma}_{pp'}^{\text{NLO}}(\hat{s}) + \hat{\sigma}_{\text{app},pp'}^{\text{NNLO}}(\hat{s}) \rightarrow \hat{\sigma}_{pp'}^{\text{NNLO}}(\hat{s}) \quad (2.3)$$

for $pp' = q\bar{q}$, where $\hat{\sigma}_{pp'}^{\text{NNLO}}(\hat{s})$ is simply the full fixed-order NNLO cross section as given in [9], now including all lower orders, and the full renormalization and factorization scale dependence [20].² In the following this implementation will be used and denoted NNLL. Note, however, that we keep the labels NNLO_{app} and NNLL₂ for the LHC even though the full $q\bar{q}$ channel is included as well, since at the LHC the gg channel dominates and the effect of the replacement in (2.3) is very small.

The theoretical uncertainties will be computed as detailed in [1] with two modifications: (1) In the $q\bar{q}$ channel the theoretical uncertainty associated with the unknown NNLO result parameterized by the estimate of a constant term in the threshold expansion has become irrelevant. This uncertainty is now included only for the gg channel. (2) Since we now include different PDF sets, we present the PDF+ α_s error at the 68% rather than 90% confidence level (CL).

2.2 Tevatron results

Since top pairs in $p\bar{p}$ collisions at the Tevatron are produced predominantly through the $q\bar{q}$ initial state, we are now in the position to present a (nearly complete) NNLL result matched to the (nearly complete) NNLO fixed-order calculation. We update our results from [1] using the same top-quark pole mass $m_t = 173.3 \text{ GeV}$ and MSTW2008NNLO [10] PDF input with $\alpha_s(M_Z) = 0.1171_{-0.0014}^{+0.0014}$ [21]. We compare the various approximations in Table 1. The NLO, NNLO_{app} and NNLL₂ entries are the same as in [1] except for the PDF+ α_s error which is now given at 68% rather than 90% CL. With the new NNLO result for the $q\bar{q}$ channel included (second line in the Table), the cross section is reduced by about 1%.³ The theoretical uncertainty of the resummed cross section from scale and

¹This result was denoted NNLL₂ in [1]. A second matching option, denoted NNLL₁, was also considered. Since this implementation is no longer useful, once the exact NNLO result is known, we do not discuss it in the present paper.

²Note that in the expressions for $f_{q\bar{q}}^{21}$ and $f_{q\bar{q}}^{22}$ in Eqs. (A1) and (A2) of [20], the functions $f_{q\bar{q}}^{(0)}$ multiplying the $n_f^{0,1}$ terms must be replaced by their threshold limit.

³Note that the difference between NNLO and NNLO_{app} on the one hand, and NNLL and NNLL₂ on the other is not exactly the same, since we recompute the value of β_{cut} in the resummation method 2, see [1], which changes from 0.35 for NNLL₂ to 0.38 for NNLL.

NLO	NNLO _{app}	NNLL ₂
6.68 ^{+0.36+0.23} _{-0.75-0.22}	7.06 ^{+0.24+0.10+0.29} _{-0.33-0.10-0.24}	7.22 ^{+0.29+0.10+0.30} _{-0.46-0.10-0.25}
	7.00 ^{+0.21+0.02+0.29} _{-0.31-0.02-0.25}	7.15 ^{+0.21+0.02+0.30} _{-0.20-0.02-0.25}
	NNLO	NNLL

Table 1: The total top-pair cross section (in pb) for $m_t = 173.3$ GeV in $p\bar{p}$ collisions at the Tevatron ($\sqrt{s} = 1.96$ TeV) with MSTW2008NNLO (NLO for NLO) input. The first set of errors refers to scale variation (scale variation+resummation ambiguities for NNLL₂ and NNLL), the last to the 68% CL PDF+ α_s error. The second set of errors for NNLO_(app)/NNLL₍₂₎ arises from variations of the unknown NNLO constant term.

resummation ambiguities and the unknown constant is reduced from $\pm 5.4\%$ to $\pm 2.9\%$. The reduction of the error from NNLO_{app} to NNLO is smaller which we attribute to the fact that a non-negligible part of the scale uncertainty originates from the gluon-gluon initial state (see Table 5 in [1]) so a further reduction is expected from the full NNLO calculation for all initial states. The smallness of the correction shows *a posteriori* that the threshold approximation works rather well (though, partly, by a fortuitous cancellation in the large β region, see [9]). Our best result for the Tevatron $t\bar{t}$ production cross section, assuming $m_t = 173.3$ GeV and $\alpha_s(M_Z) = 0.1171$, is therefore

$$\sigma_{t\bar{t}} = 7.15^{+0.21}_{-0.20} \text{ (theory)}^{+0.30}_{-0.25} \text{ (PDF}+\alpha_s) \text{ pb} \quad \text{(MSTW2008NNLO)}. \quad (2.4)$$

The cross section increases to 7.26 pb, see Table 6 below, when the “world average” value $\alpha_s(M_Z) = 0.1180$ is used. We estimate the theory uncertainty by adding the errors from scale variation, resummation ambiguities and the estimate of the constant NNLO term in the gluon channel in quadrature, where the latter has negligible effect at the Tevatron. Table 2 provides the corresponding results in the range $m_t = 165$ – 180 GeV.

It is instructive to compare the effect of adding the full NNLO $q\bar{q}$ partonic cross section to the previous NNLL resummations in the momentum-space or SCET-based resummation formalism employed here and in [1], and to the Mellin-space formalism [4, 5]. This is particularly so as the Mellin-space result as well as the result from [6] have been somewhat lower than those given in [1], see the comparison [22]. For the central values, we find

$$\begin{aligned} 7.22 \text{ pb ([1])} &\rightarrow 7.15 \text{ pb (Eq. (2.4))} && \text{(momentum-space),} \\ 6.72 \text{ pb ([4])} &\rightarrow 7.07 \text{ pb ([9])} && \text{(Mellin-space),} \end{aligned}$$

for identical m_t , α_s and PDF input. We observe that the two approaches are now in full agreement, and that the momentum-space result has turned out to be substantially less sensitive to the inclusion of the full NNLO $q\bar{q}$ channel than the Mellin-space one⁴.

⁴This is partly due to the change in the matching procedure in the Mellin-space results (from

Table 2: Total cross sections in pb at the Tevatron for $m_t = 165\text{--}180$ GeV. See caption of Table 1 for the definition of the various errors.

m_t [GeV]	NLO	NNLO	NNLL
165	8.70 ^{+0.48+0.30} _{-0.98-0.30}	9.10 ^{+0.27+0.04+0.38} _{-0.40-0.04-0.32}	9.29 ^{+0.29+0.04+0.40} _{-0.26-0.04-0.33}
166	8.42 ^{+0.46+0.29} _{-0.95-0.29}	8.82 ^{+0.26+0.03+0.37} _{-0.38-0.03-0.31}	9.00 ^{+0.28+0.03+0.38} _{-0.25-0.03-0.32}
167	8.16 ^{+0.45+0.28} _{-0.92-0.28}	8.54 ^{+0.25+0.03+0.36} _{-0.37-0.03-0.30}	8.71 ^{+0.27+0.03+0.37} _{-0.24-0.03-0.31}
168	7.90 ^{+0.43+0.27} _{-0.89-0.27}	8.27 ^{+0.25+0.03+0.35} _{-0.36-0.03-0.29}	8.44 ^{+0.26+0.03+0.36} _{-0.24-0.03-0.30}
169	7.65 ^{+0.42+0.26} _{-0.86-0.26}	8.01 ^{+0.24+0.03+0.33} _{-0.35-0.03-0.28}	8.18 ^{+0.25+0.03+0.34} _{-0.23-0.03-0.29}
170	7.41 ^{+0.40+0.26} _{-0.84-0.25}	7.76 ^{+0.23+0.03+0.32} _{-0.34-0.03-0.27}	7.92 ^{+0.24+0.03+0.33} _{-0.22-0.03-0.28}
171	7.18 ^{+0.39+0.25} _{-0.81-0.24}	7.52 ^{+0.22+0.03+0.31} _{-0.33-0.03-0.26}	7.68 ^{+0.23+0.03+0.32} _{-0.22-0.03-0.27}
172	6.96 ^{+0.38+0.24} _{-0.78-0.23}	7.29 ^{+0.22+0.03+0.30} _{-0.32-0.03-0.25}	7.44 ^{+0.22+0.03+0.31} _{-0.21-0.03-0.26}
173	6.74 ^{+0.37+0.23} _{-0.76-0.23}	7.07 ^{+0.21+0.02+0.29} _{-0.31-0.02-0.24}	7.21 ^{+0.21+0.02+0.30} _{-0.20-0.02-0.25}
174	6.54 ^{+0.35+0.23} _{-0.74-0.22}	6.85 ^{+0.20+0.02+0.28} _{-0.30-0.02-0.23}	6.99 ^{+0.21+0.02+0.29} _{-0.20-0.02-0.24}
175	6.34 ^{+0.34+0.22} _{-0.71-0.21}	6.64 ^{+0.20+0.02+0.27} _{-0.29-0.02-0.22}	6.78 ^{+0.20+0.02+0.28} _{-0.19-0.02-0.23}
176	6.14 ^{+0.33+0.21} _{-0.69-0.20}	6.44 ^{+0.19+0.02+0.26} _{-0.29-0.02-0.22}	6.57 ^{+0.19+0.02+0.27} _{-0.19-0.02-0.22}
177	5.96 ^{+0.32+0.21} _{-0.67-0.20}	6.24 ^{+0.19+0.02+0.25} _{-0.28-0.02-0.21}	6.38 ^{+0.19+0.02+0.26} _{-0.18-0.02-0.22}
178	5.78 ^{+0.31+0.20} _{-0.65-0.19}	6.06 ^{+0.18+0.02+0.25} _{-0.27-0.02-0.20}	6.18 ^{+0.18+0.02+0.25} _{-0.18-0.02-0.21}
179	5.60 ^{+0.30+0.20} _{-0.63-0.18}	5.87 ^{+0.17+0.02+0.24} _{-0.26-0.02-0.20}	6.00 ^{+0.17+0.02+0.25} _{-0.17-0.02-0.20}
180	5.43 ^{+0.29+0.19} _{-0.61-0.18}	5.70 ^{+0.17+0.02+0.23} _{-0.25-0.02-0.19}	5.82 ^{+0.17+0.02+0.24} _{-0.17-0.02-0.20}

Furthermore, the comparison to the full NNLO result shows that approximate NNLO expressions obtained from integrating approximate invariant mass or one-particle inclusive distributions [6] do not lead to a better approximation than the threshold expansion.

It is interesting to study the impact of the new, almost complete, NNLO+NNLL predictions on the extraction of the pole mass of the top quark from the measured total cross section at the Tevatron. The D0 collaboration [23] extracted the pole and $\overline{\text{MS}}$ mass using several higher-order predictions of the cross section. For instance, the pole mass $m_t = 167.5^{+5.2}_{-4.7}$ GeV was obtained using the approximate NNLO calculation from [20] and MSTW2008 PDFs. We now study the impact of our updated theory predictions on the mass measurement. To this end we fit the NNLL cross section in Table 2 by a function of

NLO+NNLL in [4] to NNLO+NNLL in [9]) and the different treatment of the NNLO constant term in [1] and [4].

the form

$$\sigma_{t\bar{t}}^{\text{th}}(m_t) = \left(\frac{172.5}{m_t}\right)^4 (c_0 + c_1(m_t - 172.5) + c_2(m_t - 172.5)^2 + c_3(m_t - 172.5)^3) \text{ pb}, \quad (2.5)$$

where all the masses are given in GeV. For the coefficients in the fit (2.5) we find $c_0 = 7.325 \pm 0.219 \pm 0.304$, $c_1 = -(5.8651 \pm 0.3163 \pm 0.3382) \times 10^{-2}$, $c_2 = (2.4884 \pm 0.7131 \pm 0.9027) \times 10^{-4}$, $c_3 = (3.7436 \pm 4.1254 \pm 1.9924) \times 10^{-6}$ where the first error denotes the total theory error and the second the PDF+ α_s error. The maximum of the positive and negative errors has been used in the fit. An analogous fit for the dependence of the experimental cross section on the reference mass is given by the D0 collaboration in [24] for the combination of the dilepton and lepton+jet results that corresponds to $\sigma_{t\bar{t}} = 7.56_{-0.56}^{+0.63}$ pb for a reference mass of $m_t = 172.5$ GeV. As in [1] the most probable value of the pole mass is obtained by the maximization of a joined likelihood function obtained from a convolution of two normalized Gaussians centered at the theoretical prediction and the experimental mean value, respectively, and with a width given by the corresponding errors. This method is similar to the one used in [23], however, we do not introduce separate likelihood functions for scale and PDF uncertainty, but add theory and PDF errors linearly. Using our best NNLL prediction, we obtain⁵

$$m_t = 171.4_{-5.7}^{+5.4} \text{ GeV}. \quad (2.6)$$

This result is in good agreement with the combined result $m_t = 173.2 \pm 0.8$ GeV from the direct mass determination at the Tevatron [25] as well as our previous result [1] $m_t = 169.8_{-4.7}^{+4.9}$ GeV using an ATLAS cross-section measurement [26] and the value $m_t = 170.3_{-6.7}^{+7.3}$ GeV obtained from a CMS cross-section measurement [27] using the calculation of [20]. In (2.6) the mass used in the kinematic reconstruction of the top-events is identified with the pole mass. Allowing for a difference of ± 1 GeV in the two mass definitions leads to an additional uncertainty of 0.5 GeV. To study the effect of the exact NNLO result of [9] and of NNLL resummation, we have repeated the same procedure for the approximate NNLO results presented in [1] and the NNLO results in Table 2. We obtain $m_t = 171.0_{-6.3}^{+5.8}$ for the approximate NNLO calculation and $m_t = 170.5_{-6.4}^{+5.7}$ for the full NNLO result, respectively. Consistent with Table 1, the effect of the result of [9] on the NNLO calculation is moderate, while a stronger reduction of the error is observed for the NNLL prediction.

2.3 LHC results

In this section we provide predictions for the top-antitop total cross section, computed with TOPIXS, for the LHC with the current centre-of-mass energy of 8 TeV, extending

⁵The uncertainty is not improved compared to [23] that used selection criteria resulting in a weaker m_t -dependence of the experimental cross section than in [24], but a larger cross section measurement of $\sigma_{t\bar{t}} = 8.13_{-0.90}^{+1.02}$ pb for a reference mass of $m_t = 172.5$ GeV. Naively rescaling the mass-dependence of the experimental cross section in [23] to the combined central value and error of [24] we obtain $m_t = 171.6_{-4.3}^{+4.3}$ GeV which might indicate the precision that could be achieved with the Tevatron data.

Table 3: Total cross sections in pb at the LHC ($\sqrt{s} = 7$ TeV) for $m_t = 165$ –180 GeV. See caption of Table 1 for the definition of the various errors.

m_t [GeV]	NLO	NNLO _{app}	NNLL ₂
165	203.9 ^{+25.5+8.6} _{-27.4-7.8}	207.4 ^{+13.6+5.7+9.2} _{-14.0-5.7-8.5}	209.4 ^{+6.6+5.7+9.3} _{-6.9-5.7-8.6}
166	197.7 ^{+24.7+8.4} _{-26.5-7.6}	201.1 ^{+13.1+5.5+8.9} _{-13.6-5.5-8.2}	202.9 ^{+6.4+5.5+9.0} _{-6.7-5.5-8.3}
167	191.6 ^{+23.9+8.1} _{-25.7-7.4}	195.0 ^{+12.7+5.3+8.6} _{-13.1-5.3-8.0}	196.8 ^{+6.3+5.3+8.7} _{-6.5-5.3-8.1}
168	185.8 ^{+23.1+7.9} _{-24.9-7.2}	189.0 ^{+12.2+5.1+8.4} _{-12.7-5.1-7.8}	190.8 ^{+6.1+5.1+8.5} _{-6.3-5.1-7.9}
169	180.2 ^{+22.4+7.7} _{-24.2-7.0}	183.3 ^{+11.8+5.0+8.1} _{-12.3-5.0-7.5}	185.0 ^{+5.9+5.0+8.3} _{-6.1-5.0-7.6}
170	174.7 ^{+21.7+7.5} _{-23.4-6.8}	177.8 ^{+11.4+4.8+7.9} _{-11.9-4.8-7.3}	179.5 ^{+5.7+4.8+8.0} _{-5.9-4.8-7.4}
171	169.5 ^{+21.0+7.2} _{-22.7-6.6}	172.5 ^{+11.0+4.6+7.7} _{-11.5-4.6-7.1}	174.1 ^{+5.5+4.6+7.8} _{-5.8-4.6-7.2}
172	164.4 ^{+20.3+7.0} _{-22.0-6.4}	167.4 ^{+10.7+4.5+7.5} _{-11.1-4.5-6.9}	168.9 ^{+5.4+4.5+7.6} _{-5.6-4.5-7.0}
173	159.6 ^{+19.7+6.8} _{-21.4-6.2}	162.4 ^{+10.3+4.3+7.3} _{-10.8-4.3-6.7}	163.9 ^{+5.2+4.3+7.4} _{-5.4-4.3-6.8}
174	154.8 ^{+19.1+6.6} _{-20.7-6.1}	157.6 ^{+10.0+4.2+7.1} _{-10.5-4.2-6.5}	159.1 ^{+5.1+4.2+7.3} _{-5.3-4.2-6.6}
175	150.3 ^{+18.5+6.5} _{-20.1-5.9}	153.0 ^{+9.7+4.1+6.9} _{-10.1-4.1-6.4}	154.4 ^{+4.9+4.1+7.0} _{-5.1-4.1-6.4}
176	145.9 ^{+17.9+6.3} _{-19.5-5.7}	148.5 ^{+9.4+3.9+6.7} _{-9.8-3.9-6.2}	149.9 ^{+5.3+3.9+6.8} _{-5.0-3.9-6.3}
177	141.6 ^{+17.4+6.1} _{-19.0-5.6}	144.2 ^{+9.1+3.8+6.5} _{-9.5-3.8-6.0}	145.5 ^{+4.6+3.8+6.6} _{-4.9-3.8-6.1}
178	137.5 ^{+16.9+5.9} _{-18.4-5.4}	140.0 ^{+8.8+3.7+6.3} _{-9.2-3.7-5.9}	141.3 ^{+4.5+3.7+6.4} _{-4.7-3.7-5.9}
179	133.5 ^{+16.3+5.8} _{-17.9-5.3}	136.0 ^{+8.5+3.6+6.1} _{-8.9-3.6-5.7}	137.3 ^{+4.4+3.6+6.2} _{-4.6-3.6-5.8}
180	129.7 ^{+15.9+5.6} _{-17.3-5.1}	132.1 ^{+8.2+3.5+6.0} _{-8.7-3.5-5.5}	133.3 ^{+4.3+3.5+6.1} _{-4.5-3.5-5.6}

the results for 7 and 14 TeV given in [1] (the result for $m_t = 173.3$ GeV with the setup of [1] was already presented in [28]). We also update the results for 7 TeV centre-of-mass energy by including the full NNLO result for the $q\bar{q}$ -initial state, although the effect on the central value is negligible since $t\bar{t}$ production at the LHC is dominated by the gluon-fusion channel where the full NNLO corrections are not known yet. Since the LHC centre-of-mass energy after the 2013–2014 shutdown has not been fixed, we do not give results for higher centre-of-mass energies. Results for other centre-of-mass energies can be easily obtained with TOPIXS since \sqrt{s} can be freely chosen in the configuration file, see the Appendix. Our best result for the $t\bar{t}$ production cross section at the LHC, using $m_t = 173.3$ GeV, the MSTW2008 PDF sets [10] and $\alpha_s(M_Z) = 0.1171$, is given by

$$\sigma_{t\bar{t}}(\text{LHC}, 7 \text{ TeV}) = 162.4_{-6.9}^{+6.7} (\text{theory})_{-6.8}^{+7.3} (\text{PDF} + \alpha_s) \text{ pb} \quad (\text{MSTW2008NNLO}) \quad (2.7)$$

$$\sigma_{t\bar{t}}(\text{LHC}, 8 \text{ TeV}) = 231.8_{-9.9}^{+9.6} (\text{theory})_{-9.1}^{+9.8} (\text{PDF} + \alpha_s) \text{ pb} \quad (\text{MSTW2008NNLO}) \quad (2.8)$$

Table 4: Total cross sections in pb at the LHC ($\sqrt{s} = 8$ TeV) for $m_t = 165$ – 180 GeV. See caption of Table 1 for the definition of the various errors.

m_t [GeV]	NLO	NNLO _{app}	NNLL ₂
165	290.1 ^{+36.1+11.7} _{-38.1-10.4}	294.5 ^{+20.0+8.3+12.3} _{-20.1-8.3-11.4}	297.0 ^{+9.1+8.3+12.4} _{-9.6-8.3-11.5}
166	281.4 ^{+35.0+11.4} _{-37.0-10.1}	285.7 ^{+19.4+8.0+12.0} _{-19.5-8.0-11.0}	288.1 ^{+8.9+8.0+12.1} _{-9.3-8.0-11.2}
167	273.0 ^{+33.9+11.1} _{-35.9-9.8}	277.2 ^{+18.7+7.8+11.6} _{-18.8-7.8-10.7}	279.5 ^{+8.6+7.8+11.8} _{-9.1-7.8-10.9}
168	264.9 ^{+32.8+10.8} _{-34.8-9.6}	269.0 ^{+18.1+7.5+11.2} _{-18.3-7.5-10.4}	271.2 ^{+8.4+7.5+11.4} _{-8.8-7.5-10.6}
169	257.0 ^{+31.8+10.4} _{-33.7-9.3}	261.0 ^{+17.5+7.3+11.0} _{-17.7-7.3-10.2}	263.2 ^{+8.1+7.3+11.1} _{-8.6-7.3-10.3}
170	249.5 ^{+30.8+10.2} _{-32.7-9.0}	253.3 ^{+17.0+7.0+10.7} _{-17.1-7.0-9.9}	255.5 ^{+7.9+7.0+10.8} _{-8.3-7.0-10.0}
171	242.1 ^{+29.9+9.9} _{-31.8-8.8}	245.9 ^{+16.4+6.8+10.4} _{-16.6-6.8-9.6}	248.0 ^{+7.6+6.8+10.5} _{-8.1-6.8-9.7}
172	235.1 ^{+29.0+9.6} _{-30.8-8.6}	238.8 ^{+15.9+6.6+10.1} _{-16.1-6.6-9.3}	240.8 ^{+7.4+6.6+10.2} _{-7.9-6.6-9.4}
173	228.3 ^{+28.1+9.3} _{-29.9-8.3}	231.9 ^{+15.4+6.4+9.8} _{-15.6-6.4-9.1}	233.9 ^{+7.2+6.4+9.9} _{-7.6-6.4-9.2}
174	221.7 ^{+27.3+9.1} _{-29.1-8.1}	225.2 ^{+14.9+6.2+9.5} _{-15.1-6.2-8.8}	227.1 ^{+7.0+6.2+9.7} _{-7.4-6.2-8.9}
175	215.3 ^{+26.4+8.8} _{-28.2-7.9}	218.7 ^{+14.4+6.0+9.3} _{-14.6-6.0-8.6}	220.6 ^{+6.8+6.0+9.4} _{-7.2-6.0-8.7}
176	209.1 ^{+25.6+8.6} _{-27.4-7.7}	212.5 ^{+14.0+5.8+9.0} _{-14.2-5.8-8.4}	214.3 ^{+6.6+5.8+9.1} _{-7.0-5.8-8.5}
177	203.2 ^{+24.9+8.3} _{-26.6-7.5}	206.4 ^{+13.5+5.6+8.8} _{-13.8-5.6-8.1}	208.2 ^{+6.4+5.6+8.9} _{-6.8-5.6-8.2}
178	197.4 ^{+24.1+8.1} _{-25.9-7.3}	200.6 ^{+13.1+5.5+8.6} _{-13.3-5.5-7.9}	202.3 ^{+6.2+5.5+8.7} _{-6.7-5.5-8.0}
179	191.8 ^{+23.4+7.9} _{-25.1-7.1}	194.9 ^{+12.7+5.3+8.3} _{-12.9-5.3-7.7}	196.6 ^{+6.1+5.3+8.4} _{-6.5-5.3-7.8}
180	186.4 ^{+22.7+7.7} _{-24.4-6.9}	189.5 ^{+12.3+5.1+8.1} _{-12.6-5.1-7.5}	191.1 ^{+5.9+5.1+8.2} _{-6.3-5.1-7.6}

The NLO, NNLO and NNLL $t\bar{t}$ cross sections at the LHC with $\sqrt{s} = 7, 8$ TeV for the mass range $m_t = 165$ – 180 GeV are shown in Table 3 and 4, respectively. The effect of corrections beyond the next-to-leading order at the LHC with $\sqrt{s} = 8$ TeV is similar to that observed for $\sqrt{s} = 7$ TeV, increasing the cross section by 2.4% compared to the NLO result, with fixed-order NNLO contributions accounting for 1.6%. It can be seen from Tables 3 and 4 that the uncertainty from the unknown fixed-order NNLO corrections for the gg (and qg) initial states, as estimated by the variation of the constant term in the threshold expansion, are of the same order as the remaining theory errors of the NNLL results at the LHC. This source of uncertainty will be removed once the full NNLO calculation has been performed also for these channels⁶.

Comparing to our previous predictions for the LHC with $\sqrt{s} = 7$ TeV [1] and $\sqrt{s} =$

⁶For recent work constraining the NNLO cross section using information on the $\beta \rightarrow 1$ or large invariant-mass limits, see [29, 30].

Table 5: Values for β_{cut} . The strong coupling constant is $\alpha_s(M_Z) = 0.118$.

PDF set	Tevatron			LHC7			LHC8		
	$k_s = 1$	2	4	$k_s = 1$	2	4	$k_s = 1$	2	4
MSTW2008	0.56	0.38	0.34	0.74	0.54	0.33	0.76	0.54	0.33
NNPDF2.1	0.53	0.29	0.19	0.74	0.51	0.25	0.75	0.52	0.25
ABM11	0.54	0.36	0.22	0.73	0.54	0.33	0.74	0.54	0.33
CT10	0.57	0.39	0.24	0.74	0.54	0.33	0.75	0.54	0.33

8 TeV [28] it is seen that in our approach the inclusion of the exact NNLO result for the $q\bar{q}$ channel amounts to a minimal change of the central value by $-(0.1-0.2)$ pb:

$$162.6 \text{ pb ([1])} \rightarrow 162.4 \text{ pb (Eq. (2.7))} \quad (7 \text{ TeV}),$$

$$231.9 \text{ pb ([28])} \rightarrow 231.8 \text{ pb (Eq. (2.8))} \quad (8 \text{ TeV}).$$

The effect on the theory error is somewhat larger and we find a reduction from $^{+7.4}_{-7.6}$ to $^{+6.7}_{-6.9}$ pb at $\sqrt{s} = 7$ TeV and from $^{+10.5}_{-10.3}$ to $^{+9.6}_{-9.9}$ pb at $\sqrt{s} = 8$ TeV. Again, a larger effect on the central value is observed in the approach of [4, 5]:⁷

$$158.7 \text{ pb ([4])} \rightarrow 156.2 \text{ pb ([5])} \quad (7 \text{ TeV}),$$

$$226.6 \text{ pb ([4])} \rightarrow 222.5 \text{ pb ([5])} \quad (8 \text{ TeV}).$$

While these results agree with ours within the quoted uncertainties, the relative difference is larger than for the Tevatron which indicates the relevance of the uncalculated fixed-order NNLO terms for the dominant gluon-fusion channel.

3 Dependence on PDF sets

In this section we present results for the cross section computed with different PDF sets. As representatives we choose MSTW2008 [10], NNPDF2.1 [31], ABM11 [11], and CT10 [32]. (Note that CT10 at the moment provides only NLO PDFs.) We use $m_t = 173.3$ GeV, and choose PDF sets for the common value $\alpha_s(M_Z) = 0.118$ of the strong coupling constant. This provides complementary information to [11], where results for different PDF sets with their best, but often rather different α_s values have been presented, which, due to the dependence of the partonic cross sections on α_s , obscures the difference due to the parton densities themselves.

⁷When comparing the NNLO_{app} results from TOPIXS to those obtained with top++1.2 [5] one finds a small difference of 0.1–0.3 pb. This is due to the implementation of the approximate NNLO corrections for the gg initial state, where the exact tree cross sections for the separate colour-singlet and octet channels are used in TOPIXS, while the colour averaged tree cross sections are used in top++. In the threshold limit both implementations agree, so they are formally of the same accuracy.

Table 6: Total cross sections in pb at the Tevatron and LHC ($\sqrt{s} = 7$ TeV and 8 TeV for different PDF sets and common strong coupling input $\alpha_s(M_Z) = 0.118$. See caption of Table 1 for the definition of the various errors.

Tevatron	NLO	NNLO	NNLL
MSTW2008	6.48 ^{+0.33+0.23} _{-0.70-0.22}	7.11 ^{+0.22+0.03+0.29} _{-0.32-0.03-0.24}	7.26 ^{+0.22+0.03+0.30} _{-0.21-0.03-0.25}
NNPDF2.1	6.77 ^{+0.34+0.23} _{-0.62-0.23}	7.18 ^{+0.22+0.02+0.26} _{-0.17-0.02-0.26}	7.49 ^{+0.26+0.02+0.27} _{-0.25-0.02-0.27}
ABM11	6.45 ^{+0.26+0.14} _{-0.64-0.14}	7.29 ^{+0.22+0.01+0.15} _{-0.31-0.01-0.15}	7.46 ^{+0.22+0.01+0.16} _{-0.20-0.01-0.16}
CT10	6.75 ^{+0.35+0.46} _{-0.74-0.35}	7.33 ^{+0.22+0.03+0.52} _{-0.33-0.03-0.40}	7.47 ^{+0.23+0.03+0.52} _{-0.22-0.03-0.41}
LHC7	NLO	NNLO _{app}	NNLL ₂
MSTW2008	151.8 ^{+18.2+6.8} _{-19.9-6.2}	164.3 ^{+10.6+4.4+7.2} _{-11.1-4.4-6.7}	165.9 ^{+5.3+4.4+7.3} _{-5.6-4.4-6.8}
NNPDF2.1	157.0 ^{+19.1+6.8} _{-19.7-6.8}	161.9 ^{+8.3+4.3+7.1} _{-7.5-4.3-7.1}	166.1 ^{+7.0+4.3+7.3} _{-8.3-4.3-7.3}
ABM11	123.3 ^{+14.5+5.0} _{-16.1-5.0}	146.7 ^{+9.4+3.8+5.8} _{-9.7-3.8-5.8}	148.2 ^{+5.3+3.8+5.9} _{-5.3-3.8-5.9}
CT10	148.7 ^{+17.7+12.7} _{-19.3-11.4}	160.7 ^{+10.4+4.4+13.6} _{-10.8-4.4-12.2}	162.3 ^{+5.2+4.4+13.7} _{-5.4-4.4-12.3}
LHC8	NLO	NNLO _{app}	NNLL ₂
MSTW2008	217.5 ^{+26.0+9.2} _{-27.9-8.3}	234.4 ^{+15.7+6.5+9.7} _{-16.0-6.5-9.0}	236.5 ^{+7.4+6.5+9.8} _{-7.3-6.5-9.1}
NNPDF2.1	225.1 ^{+27.3+9.0} _{-27.6-9.0}	232.2 ^{+12.2+6.5+9.4} _{-11.0-6.5-9.4}	238.0 ^{+9.7+6.5+9.7} _{-11.7-6.5-9.7}
ABM11	180.8 ^{+21.4+6.8} _{-23.3-6.8}	212.1 ^{+14.2+5.7+7.8} _{-14.3-5.7-7.8}	214.1 ^{+7.4+5.7+7.9} _{-7.2-5.7-7.9}
CT10	212.8 ^{+25.3+16.5} _{-27.1-14.8}	229.2 ^{+15.5+6.4+17.6} _{-15.6-6.4-15.8}	231.2 ^{+7.2+6.4+17.7} _{-7.2-6.4-15.9}

For NNPDF2.1 the total number of replicas used is $N_{\text{rep}} = 100$. To determine the PDF+ α_s error, this number is distributed over sets with different α_s values according to a Gaussian distribution with a standard deviation of $\delta\alpha_s = 0.0015$. For MSTW2008 and CT10 we provide asymmetric PDF+ α_s errors using the methods from [21,33]. In the latter case we use $\delta\alpha_s = 0.002$ as the standard deviation. For ABM11 we compute symmetric errors with the formula

$$\delta\sigma = \sqrt{\sum_k (\sigma_0 - \sigma_k)^2}, \quad (3.1)$$

where the sum runs over all eigenvectors of the given set. This is the same prescription as in [11]. Note that in the case of ABM11 α_s is one of the parameters of the fit. Thus, the PDF error computed above already includes the uncertainty due to the variation of the strong coupling constant. For the NNLL calculation we also have to determine the parameter β_{cut} . The values are given in Table 5.

The results for the cross section at the Tevatron and at the LHC with $\sqrt{s} = 7$ TeV and $\sqrt{s} = 8$ TeV are given in Table 6.⁸ We find good agreement between the different PDF sets for the cross section at the Tevatron. At the LHC, we find again agreement between MSTW2008, NNPDF2.1, and CT10, but the value of ABM11 is significantly lower than the others. This reflects the smaller gluon density in the ABM11 fit that does not make use of the Tevatron jet data, which drive the high- x gluon distribution upwards. The difference in the top cross section is significantly larger than the error assigned to the individual PDF fits, which indicates that it may be possible to use the top-pair production cross section to constrain the gluon density. We pursue this further in Section 5.

4 Heavy “top” quarks

Heavy colour-triplet fermions appear in the extension of the standard model by a fourth generation, and are also often introduced to cancel the top-loop contributions to the Higgs mass in non-supersymmetric models that aim at addressing the hierarchy problem (such as Little Higgs models [34, 35]). In this context the extra fermions can be singlets under the $SU(2)_L$ gauge group or may transform under non-chiral representations, so they are less constrained than fourth generation quarks. Heavy colour-triplet fermions in other $SU(2)_L$ representations with exotic electric charges have also been introduced in models of electroweak symmetry breaking [36]. Within QCD, the production cross sections of these postulated particles only depend on the spin and colour charge and can be computed with TOPIXS.

The LHC experiments have already performed direct searches for the production of heavy quarks in various decay channels, with the most stringent bounds $m_B > 611$ GeV (for a heavy bottom quark B decaying exclusively as $B \rightarrow tW$, using 4.7 fb^{-1} of data [37]), $m_T > 557$ GeV (for a heavy top quark decaying exclusively as $T \rightarrow bW$, using 5.0 fb^{-1} of data [38]), $m_T > 475$ GeV (for the decay $T \rightarrow tZ$ allowed for $SU(2)$ singlet T , using 1.14 fb^{-1} [39]).

In Table 7 we present our predictions for the production cross section of heavy quarks Q at the LHC with 7 TeV centre-of-mass energy for the mass range $m_Q = 350\text{--}700$ GeV that is relevant for the analysis of 5 fb^{-1} of data collected in the 2011 run, and for masses up to 1 TeV at the LHC operating at $\sqrt{s} = 8$ TeV. For each mass the value of the parameter β_{cut} appearing in the momentum-space resummation formalism with a running soft scale has been determined using the procedure introduced in [1]. The resulting values range from $\beta_{cut} = 0.50\text{--}0.42$ for $m_Q = 350\text{--}700$ GeV and $\sqrt{s} = 7$ TeV, and from $\beta_{cut} = 0.51\text{--}0.39$ for $m_Q = 350\text{--}1000$ GeV at the LHC with $\sqrt{s} = 8$ TeV, and are implemented as default values in TOPIXS. We use the MSTW2008 PDFs and the running strong coupling with five active quark flavours and therefore neglect the impact of the top quark on the evolution of these quantities. The partonic cross sections are also computed with five massless flavours,

⁸The small difference in the MSTW2008 values with respect to Section 2 is due to the different value of $\alpha_s(M_Z)$.

Table 7: Total cross sections for the production of heavy quarks Q beyond the standard model in pb at the LHC ($\sqrt{s} = 7$ TeV, upper table and $\sqrt{s} = 8$ TeV, lower table). See caption of Table 1 for the definition of the various errors. Heavy “top” mass m_Q in GeV.

LHC, $\sqrt{s} = 7$ TeV

m_Q	NLO	NNLO _{app}	NNLL ₂
350	$3.11^{+0.32+0.17}_{-0.40-0.15}$	$3.17^{+0.13+0.05+0.18}_{-0.16-0.05-0.16}$	$3.21^{+0.12+0.05+0.18}_{-0.11-0.05-0.16}$
400	$1.37^{+0.13+0.08}_{-0.17-0.07}$	$1.39^{+0.05+0.02+0.08}_{-0.07-0.02-0.07}$	$1.41^{+0.06+0.02+0.08}_{-0.05-0.02-0.07}$
450	$6.44^{+0.62+0.40}_{-0.81-0.32} \times 10^{-1}$	$6.56^{+0.23+0.09+0.40}_{-0.30-0.09-0.34} \times 10^{-1}$	$6.66^{+0.27+0.09+0.41}_{-0.24-0.09-0.34} \times 10^{-1}$
500	$3.20^{+0.30+0.21}_{-0.40-0.16} \times 10^{-1}$	$3.26^{+0.11+0.04+0.21}_{-0.14-0.04-0.17} \times 10^{-1}$	$3.32^{+0.14+0.04+0.21}_{-0.11-0.04-0.17} \times 10^{-1}$
550	$1.67^{+0.15+0.11}_{-0.21-0.09} \times 10^{-1}$	$1.70^{+0.05+0.02+0.11}_{-0.07-0.02-0.09} \times 10^{-1}$	$1.73^{+0.07+0.02+0.11}_{-0.06-0.02-0.09} \times 10^{-1}$
600	$8.97^{+0.82+0.63}_{-1.12-0.49} \times 10^{-2}$	$9.14^{+0.26+0.09+0.63}_{-0.38-0.09-0.48} \times 10^{-2}$	$9.31^{+0.40+0.09+0.64}_{-0.32-0.09-0.50} \times 10^{-2}$
650	$4.96^{+0.45+0.36}_{-0.62-0.28} \times 10^{-2}$	$5.06^{+0.14+0.04+0.37}_{-0.20-0.04-0.27} \times 10^{-2}$	$5.17^{+0.23+0.04+0.38}_{-0.18-0.04-0.28} \times 10^{-2}$
700	$2.81^{+0.25+0.22}_{-0.35-0.17} \times 10^{-2}$	$2.87^{+0.08+0.02+0.22}_{-0.11-0.02-0.16} \times 10^{-2}$	$2.94^{+0.13+0.02+0.23}_{-0.10-0.02-0.16} \times 10^{-2}$

LHC, $\sqrt{s} = 8$ TeV

m_Q	NLO	NNLO _{app}	NNLL ₂
350	$4.93^{+0.50+0.26}_{-0.62-0.23}$	$5.03^{+0.22+0.09+0.27}_{-0.26-0.09-0.24}$	$5.09^{+0.19+0.09+0.28}_{-0.18-0.09-0.24}$
400	$2.23^{+0.22+0.12}_{-0.28-0.11}$	$2.27^{+0.09+0.04+0.13}_{-0.11-0.04-0.11}$	$2.30^{+0.09+0.04+0.13}_{-0.08-0.04-0.11}$
450	$1.08^{+0.10+0.06}_{-0.13-0.05}$	$1.10^{+0.04+0.02+0.06}_{-0.05-0.02-0.05}$	$1.12^{+0.04+0.02+0.06}_{-0.04-0.02-0.06}$
500	$5.55^{+0.51+0.33}_{-0.68-0.27} \times 10^{-1}$	$5.65^{+0.19+0.07+0.34}_{-0.25-0.07-0.28} \times 10^{-1}$	$5.73^{+0.23+0.07+0.34}_{-0.20-0.07-0.29} \times 10^{-1}$
550	$2.97^{+0.27+0.19}_{-0.36-0.15} \times 10^{-1}$	$3.03^{+0.10+0.04+0.19}_{-0.13-0.04-0.15} \times 10^{-1}$	$3.07^{+0.13+0.04+0.19}_{-0.11-0.04-0.16} \times 10^{-1}$
600	$1.65^{+0.15+0.11}_{-0.20-0.08} \times 10^{-1}$	$1.68^{+0.05+0.02+0.11}_{-0.07-0.02-0.09} \times 10^{-1}$	$1.71^{+0.07+0.02+0.11}_{-0.06-0.02-0.09} \times 10^{-1}$
650	$9.44^{+0.84+0.63}_{-1.15-0.50} \times 10^{-2}$	$9.62^{+0.27+0.09+0.64}_{-0.39-0.09-0.49} \times 10^{-2}$	$9.78^{+0.41+0.09+0.65}_{-0.33-0.09-0.51} \times 10^{-2}$
700	$5.54^{+0.49+0.39}_{-0.68-0.30} \times 10^{-2}$	$5.64^{+0.16+0.05+0.39}_{-0.22-0.05-0.29} \times 10^{-2}$	$5.74^{+0.25+0.05+0.40}_{-0.19-0.05-0.30} \times 10^{-2}$
750	$3.31^{+0.29+0.24}_{-0.41-0.19} \times 10^{-2}$	$3.38^{+0.09+0.03+0.25}_{-0.13-0.03-0.18} \times 10^{-2}$	$3.44^{+0.15+0.03+0.25}_{-0.12-0.03-0.18} \times 10^{-2}$
800	$2.02^{+0.18+0.15}_{-0.25-0.12} \times 10^{-2}$	$2.06^{+0.05+0.02+0.16}_{-0.08-0.02-0.11} \times 10^{-2}$	$2.10^{+0.09+0.02+0.16}_{-0.07-0.02-0.11} \times 10^{-2}$
850	$1.25^{+0.11+0.10}_{-0.15-0.08} \times 10^{-2}$	$1.27^{+0.03+0.01+0.10}_{-0.05-0.01-0.07} \times 10^{-2}$	$1.30^{+0.06+0.01+0.11}_{-0.04-0.01-0.07} \times 10^{-2}$
900	$7.81^{+0.69+0.65}_{-0.97-0.50} \times 10^{-3}$	$7.99^{+0.20+0.05+0.69}_{-0.29-0.05-0.46} \times 10^{-3}$	$8.18^{+0.37+0.05+0.70}_{-0.26-0.05-0.47} \times 10^{-3}$
950	$4.94^{+0.44+0.43}_{-0.61-0.33} \times 10^{-3}$	$5.07^{+0.13+0.03+0.46}_{-0.18-0.03-0.30} \times 10^{-3}$	$5.19^{+0.23+0.03+0.47}_{-0.16-0.03-0.31} \times 10^{-3}$
1000	$3.15^{+0.28+0.29}_{-0.40-0.22} \times 10^{-3}$	$3.24^{+0.08+0.02+0.31}_{-0.12-0.02-0.20} \times 10^{-3}$	$3.32^{+0.15+0.02+0.32}_{-0.11-0.02-0.21} \times 10^{-3}$

which corresponds to replacing the top quark t by Q (rather than adding Q to the known quarks). The same approximation was also used in [4].

For the mass range $m_Q = 350\text{--}700$ GeV at the LHC with $\sqrt{s} = 7$ TeV, the NNLL corrections grow from about 3% to above 4% relative to the NLO cross section evaluated with the appropriate NLO PDFs, while for $m_Q = 1$ TeV at the LHC with $\sqrt{s} = 8$ TeV the NNLL corrections become larger than 5%. In this comparison, the higher-order corrections are partially compensated by the change from NLO to NNLO PDFs, with the associated change in the value of the strong coupling. Normalizing the higher-order results instead to the NLO cross section evaluated with MSTW2008NNLO PDFs, the NNLL corrections range from 10% for $m_Q = 350$ GeV to 14% for $m_Q = 1000$ GeV at the LHC with $\sqrt{s} = 8$ TeV, while the approximate NNLO cross section amounts to a 9–11% correction. Therefore higher-order effects beyond NNLO are small, but reach a magnitude of the order of the residual uncertainty of the approximate NNLO result for larger masses.

The total theoretical uncertainty defined below (2.4) is largely independent of the mass and centre-of-mass energy. At $\sqrt{s} = 8$ TeV, in the mass range $m_Q = 350\text{--}1000$ GeV, it ranges from $^{+10\%}_{-13\%}$ to $^{+9\%}_{-13\%}$ at NLO, from $^{+5\%}_{-5\%}$ to $^{+3\%}_{-4\%}$ at NNLO, and from $^{+4\%}_{-4\%}$ to $^{+5\%}_{-3\%}$ at NNLL. It is counterintuitive that for larger masses the error estimate of the approximate NNLO prediction becomes smaller than that for NNLL. However, the size of our uncertainty estimate for large masses is similar to that found in [4], so this issue is common to the Mellin-space and momentum space results. The relative PDF uncertainty is similar at NLO, NNLO_{app} and NNLL and grows from $^{+5\%}_{-5\%}$ to $^{+10\%}_{-6\%}$ for $m_Q = 350\text{--}1000$ GeV at $\sqrt{s} = 8$ TeV. Performing the computation with the NNPDF2.1 PDF set we find that the results for NNLL₂ (NNLO_{app}) are smaller by 4–6% (3%) if the same coupling constant is used for both PDF sets. Therefore both sets agree within the estimated PDF uncertainty.

Since the contribution of the threshold region to the total cross section is more important for larger masses, we expect that the ambiguities in the implementation of threshold resummation are reduced and the predictions of different formalisms show better agreement than for lighter quarks. We therefore compare our default implementation, NNLL₂, to an implementation NNLL_{fix} of resummation in momentum space with a fixed soft scale, determined using the method proposed in [19], that was denoted as “Method 1” in [1]. This implementation is available in TOPIXS with the option MUSRUN=0, and the default values of the fixed soft scale are implemented for MSTW2008 with $m_Q = 173.3\text{--}2000$ GeV. By NNLL_N we denote the results obtained using the program top++1.2 [5] that implements resummation using the traditional Mellin-moment method [4]. In Figure 1 the results of the three implementations are shown for the LHC with 8 TeV centre-of-mass energy for the mass range $m_Q = 200\text{--}1600$ GeV. The larger masses are not relevant for phenomenology with 20 fb^{-1} luminosity, but are included here in order to compare the three implementations in a regime where the threshold approximation is expected to be more accurate. We plot the quantity $K_{\text{NNLL}} = \sigma_{t\bar{t}}^{\text{NNLL}}/\sigma_{t\bar{t}}^{\text{NLO}}$, where for comparison the NLO cross section in the denominator is evaluated with the NNLO PDFs, in contrast to our default treatment. It is seen that the three implementations are in good agreement once the higher-order corrections become larger than 10%, with larger differences for smaller masses. The difference of the Mellin-space implementation to our default is always of a similar magnitude

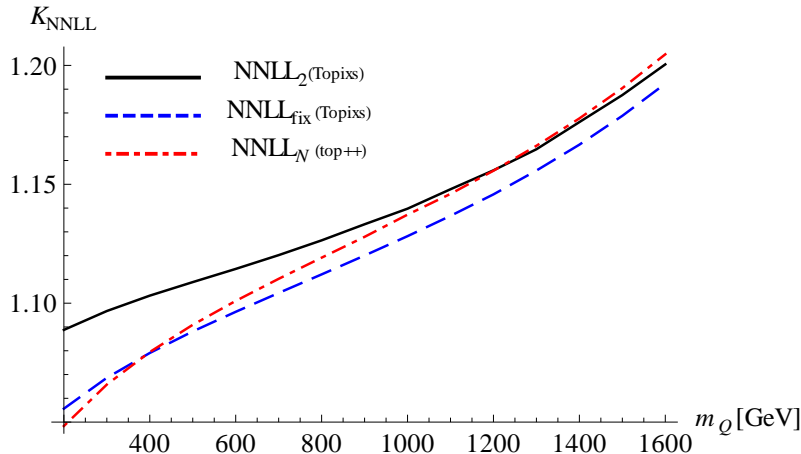


Figure 1: Comparison of the ratio $K_{\text{NNLL}} = \sigma_{t\bar{t}}^{\text{NNLL}}/\sigma_{t\bar{t}}^{\text{NLO}}$ for heavy quark production at the LHC with $\sqrt{s} = 8$ TeV for our default implementation NNLL_2 (black, solid) to our fixed-scale implementation NNLL_{fix} (blue, dashed) and the results NNLL_N (red, dot-dashed) from the Mellin-space approach [4, 5]. The NNLL results are normalized by the NLO cross section computed with NNLO PDFs.

or smaller than that of the two momentum-space implementations⁹ so we conclude that the momentum-space and Mellin-space approaches agree within the ambiguities inherent in the threshold approximation.

5 Gluon distribution function

The precise knowledge of parton distribution functions (PDFs) and of their uncertainties is a crucial requirement for the LHC physics program, particularly when the error on PDFs represents the largest single theoretical uncertainty, as is the case in top-pair production. PDFs are extracted by several collaborations [10, 11, 31, 32, 40, 41] from a large number of measurements collected at different experiments, the early fixed-target deep-inelastic scattering (DIS) and Drell-Yan (DY) experiments and the modern HERA and Tevatron colliders. In the meantime the LHC, thanks to the accumulated high statistics and the well-controlled systematics, is providing the PDF fitting collaborations with a large amount of precise data. Soon the LHC measurements are going to provide essential constraints on most PDF combinations. The NNPDF collaboration has already published a PDF analysis, NNPDF2.2, which includes early electro-weak LHC data from the 2010 runs [15].

⁹The results from TOPIXs include bound-state effects and the resummation of Coulomb corrections beyond NNLO not included in top++. However, the bound-state contribution to K_{NNLL} is of the order of 0.3–0.4 percent for the mass range considered in Figure 1, so the conclusion of the comparison to top++ is not affected. For top-pair production the contribution of the Coulomb corrections beyond NNLO above threshold was found to be even smaller [1], which we also expect to be the case for larger masses.

A recent study of the impact of LHC W lepton charge-asymmetry data on a MSTW2008 Monte Carlo parton set was presented in [42].

In this section we investigate the possibility to constrain the gluon distribution in the proton through the top-pair production cross section by combining the most accurate available theoretical calculation presented in this paper with LHC data. This is interesting in several respects. First, while the gluon distribution function at medium–small x is rather well constrained by the precise HERA measurements of the scaling of the structure functions, at medium–large x the gluon is currently constrained primarily from the jet inclusive measurements performed at the Tevatron. A more precise determination of the gluon at medium–large x , which is the region probed by the $t\bar{t}$ measurements at the LHC, would lead to an improved theoretical precision of the Higgs cross section in gluon fusion. Moreover the top-pair production cross section is correlated to the strong coupling constant and therefore potentially reduces the uncertainty in the determination of α_s from PDF global analyses.

In this section, we quantify the impact of the LHC measurements of the total $t\bar{t}$ cross section on the gluon uncertainty by using the re-weighting technique [14,15]. This technique is valid for Monte Carlo sets of PDFs, like those provided by the NNPDF collaboration. These sets determine a Monte Carlo representation of the probability density in the space of PDFs. This feature allows to include new experimental data by using Bayes’ theorem, i.e. by re-weighting an existing PDF set (prior probability) without having to perform a new fit of the entire data. The effect of a new independent dataset is quantified by computing for each replica k ($k = 1, \dots, N_{\text{rep}}$) of the starting PDF set a weight w_k , which assesses the probability that the PDF replica agrees with the new data. The re-weighted ensemble then forms a representation of the probability distribution of PDFs conditional on both the old and the new data. The weights are computed straightforwardly by evaluating the χ_k^2 of the new data to each of the replicas, according to Eq. (9) of [14]. The distribution can then be unweighted and a new PDF set, which now includes both the data fitted in the initial PDF set and the additional data, is extracted.

Before presenting the results of this analysis, it is important to specify the three ingredients that are employed in order to determine the χ_k^2 of the LHC top-pair production data to each replica and therefore the weights w_k : the experimental data, the theoretical predictions and the prior PDF set.

The (single) experimental data added to the PDF analysis is obtained from the combination of the ATLAS and CMS $t\bar{t}$ cross section measurements presented in [26, 43–45]. While the proper combination of these results can only be performed by the experimental collaborations, we simply combine them here in a single data point by adding in quadrature statistical and systematic errors of the ATLAS and CMS combined results, and by adding the luminosity errors as a 100% correlated uncertainty between the two experiments, which results in

$$\sigma_{t\bar{t}}^{\text{exp.}} = 173.23 \pm 6.55 \text{ (stat. + syst.)} \pm 7.00 \text{ (lumi.) pb} = 173.23 \pm 9.59 \text{ pb.} \quad (5.1)$$

The theoretical predictions $\sigma_{t\bar{t},k}^{\text{th}}$ are obtained for each PDF replica k from (2.2).¹⁰ Since the PDF errors do not account for theoretical uncertainties, the latter are neither included in the computation of the weights w_k . As starting PDF sets, we consider two cases. In the first part of the analysis, the prior probability is given by the NNPDF2.1 NNLO parton set. The latter is a NNLO determination of parton distributions from a global set of hard-scattering data, including DIS, Drell-Yan and jet data. Each set is determined for a given value of $\alpha_s(M_Z)$, which is treated as an external parameter. Several sets are available with $\alpha_s^j = 0.114, 0.115, \dots, 0.124$. Since the $t\bar{t}$ cross section is strongly correlated to α_s , which in turn is strongly correlated to the gluon density, it is important to take into account the α_s uncertainty in the prior PDF set. The $N_{\alpha_s}^j$ replicas determining the starting parton set (such that $\sum_{j=1}^{N_{\alpha_s}} N_{\alpha_s}^j = 350$) are taken from various α_s^j sets, as it was done in Section 3 to determine the PDF+ α_s uncertainty, according to a Gaussian distribution centered on $\alpha_s(M_Z) = 0.118$ with a standard deviation of $\delta\alpha_s = 0.0015$.

The results of the re-weighting are displayed in Figure 2. On the left-hand side the impact of including the LHC measurement on the gluon density, with $\mu_f = m_t = 173.3$ GeV, is shown. As expected, there is an effect in the large- x region. The uncertainty in the gluon density given by the width of the bands can be assessed directly from the bottom-left plot, where the two lines refer to before and after including the $t\bar{t}$ cross section in the PDF analysis. Since the $t\bar{t}$ cross section predicted with the NNPDF2.1 PDF is close to (5.1), see Table 6, there is only a small effect on the central gluon distribution. However, the uncertainty is reduced by about 20% for $x \gtrsim 0.15$. The same results are shown on the right-hand side of Figure 2 but for the gluon-gluon luminosity, defined by

$$\mathcal{L}_{gg}(\tau) = \frac{1}{s} \int_{\tau}^1 \frac{dy}{y} f_{g/p}(y, \mu_f) f_{g/p}(\tau/y, \mu_f), \quad (5.2)$$

where s is the LHC centre-of-mass energy squared and μ , following Ref. [46], is set to $\mu_f = \sqrt{\tau s}$. A similar impact as the one observed on the gluon density is observed on the gg luminosity in the expected region $\sqrt{\tau} \geq 2m_t/\sqrt{s} \sim 0.05$ and partially also in the smaller $\sqrt{\tau}$ region due to the momentum conservation sum rules. The predicted $t\bar{t}$ cross section evaluated with the NNPDF2.1 set changes from $\sigma_{t\bar{t}}^{\text{th}} = 166.1 \pm 7.0$ (PDF) pb to $\sigma_{t\bar{t}}^{\text{th}} = 168.4 \pm 5.4$ (PDF) after re-weighting; the central value gets closer to the experimental data, and the PDF uncertainty is reduced by about 25%. On top of that, we observe that the χ^2 per degree of freedom to the Tevatron jet data is reduced by the inclusion of the $t\bar{t}$ measurement. If the same analysis were performed by using as a prior set the NNPDF2.1 set with fixed α_s , the impact would be rather smaller, as the reduction of the uncertainty is not only due to the gluon, but also to $\alpha_s(M_Z)$, whose value computed over the replicas increases from 0.1180 ± 0.0015 to 0.1184 ± 0.0013 after including the $t\bar{t}$ data in the fit.

It is interesting to observe that the effect is already visible with the data collected in the 2011 7 TeV LHC run. We can then expect an even more significant effect, when in

¹⁰The present analysis has been performed before [9] appeared and hence does not include the full $q\bar{q}$ NNLO partonic cross section. However, as discussed above, this has a negligible effect on the central value of the gluon-dominated $t\bar{t}$ cross section at LHC. Since the present re-weighting analysis does not include theoretical errors, only the central value matters.

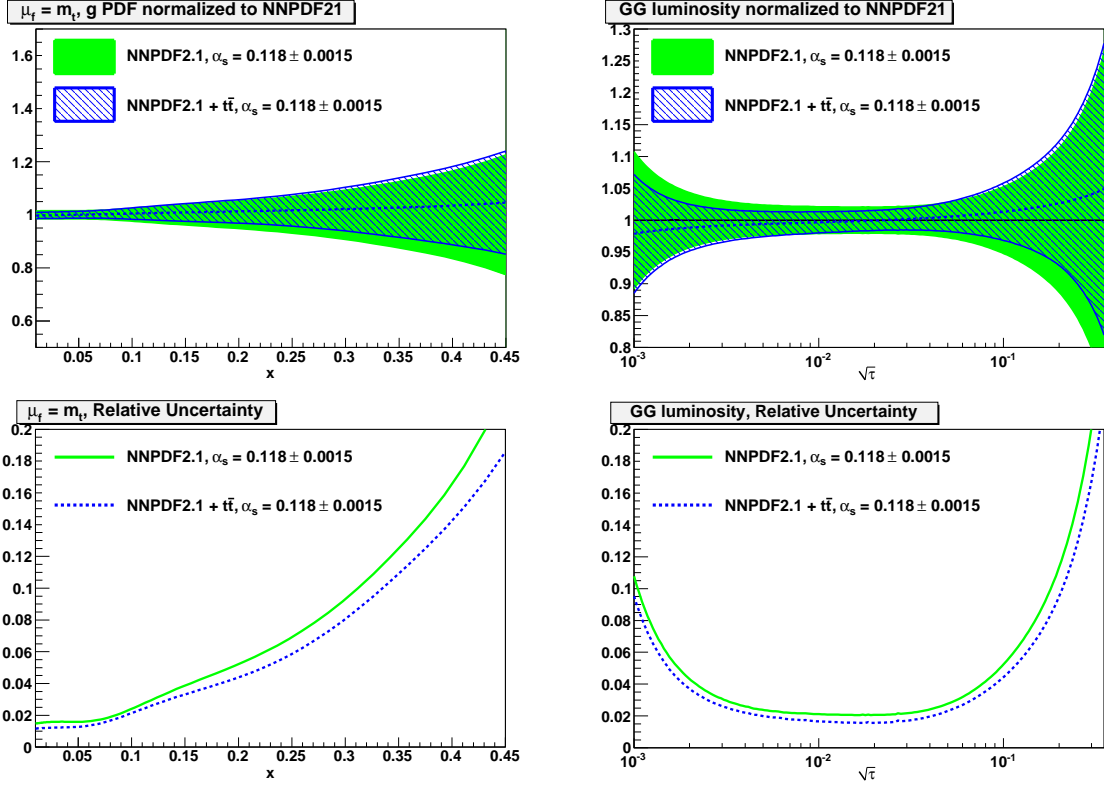


Figure 2: Effect of including the total $t\bar{t}$ cross-section measurement into the NNPDF2.1 global analysis for varying α_s . Top: Gluon distribution (left) and gg luminosity (right) before (solid, solid green in color) and after (shaded, shaded blue in color) including the $t\bar{t}$ measurement in the NNPDF fit. Both curves are normalized to the central value of the NNPDF2.1 gluon before re-weighting. Bottom: Half-width of the error bands in the upper plots before (solid, solid green in color) and after (dashed, dashed blue in color) the inclusion of the $t\bar{t}$ measurement in the fit.

the near future the experimental precision will reach the present theoretical accuracy. We therefore show in Figure 3 what happens if we suppose that the measured $t\bar{t}$ cross section had an error as large as the theoretical uncertainty,¹¹ while the central value is kept fixed,

$$\sigma_{t\bar{t}}^{\text{fake}} = 173.23_{-6.9}^{+6.7} \text{ pb}, \quad (5.3)$$

and observe a further reduction by 5% (to a total of 25%) of the uncertainty in the gluon distribution to the NNPDF2.1 gluon in the large- x region. This means that, on the one hand, the limiting factor will soon be the theoretical uncertainty, which will be reduced further only once the full NNLO gg partonic cross section is known. On the other hand, it is remarkable to see a significant effect from a single additional measurement that competes with thousands of other measurements already included in PDF global analyses, in

¹¹Here we adopt the error from the MSTW2008 PDF set in Table 6 that leads to a slightly smaller theoretical uncertainty.

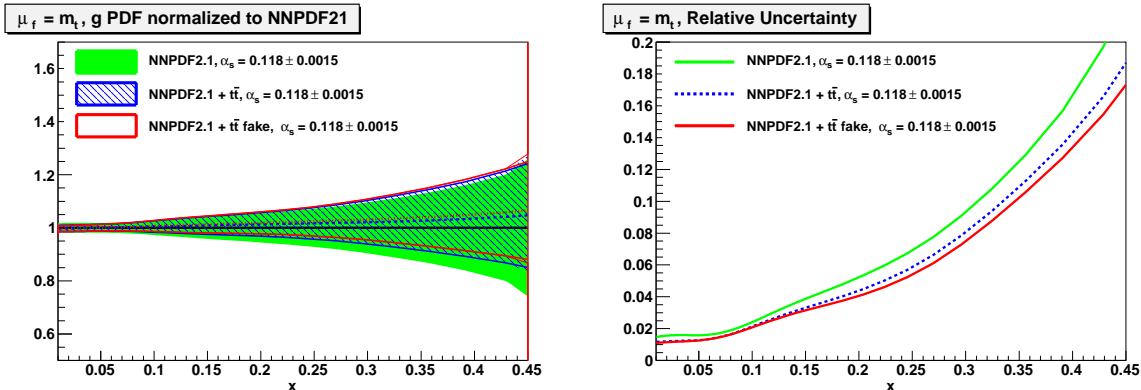


Figure 3: Effect of including the total $t\bar{t}$ cross section measurement with reduced uncertainty into the NNPDF2.1 global analysis for varying α_s . Gluon distribution (left) and (right) half-width of the gluon error band in the left plot before (solid light gray, solid green in color) and after including the $t\bar{t}$ measurement in the fit. In this case the dashed curve (dashed, dashed blue in color) refers to the inclusion of the real measurement (5.1), the solid dark gray curve (solid, solid red in color) refers to the inclusion of the measurement with reduced uncertainty (5.3).

particular with the approximately 200 inclusive jet data points collected at Tevatron Run II that are relevant in the large- x region. A larger effect should therefore be expected, once $t\bar{t}$ rapidity and invariant mass distributions will be included in the PDF fits.

In order to disentangle the effect of the jet data from the one of the top-pair production data, we now start from the NNPDF2.1.DIS+DY set as prior probability, which has the same features as the NNPDF2.1 global set, but does not contain the jet data. This implies that the PDF uncertainty of the gluon at medium–large x is larger. We can therefore assess whether the top cross section pushes the gluon into the same direction as the Tevatron jet data and compare the constraining power of top-pair production relative to the inclusive jet measurements. Furthermore, the starting PDF set is supposedly closer to the ABM11 NNLO PDF set [11], which does not include the Tevatron data, allowing us to draw some conclusion on the differences observed in Section 3 between theoretical predictions obtained with ABM11 and the other PDF sets.

The theoretical prediction for the total top-pair production cross section obtained with the NNPDF2.1.DIS+DY set is $\sigma_{t\bar{t}}^{\text{th.}} = 161.1 \pm 9.9$ (PDF) pb, 3% smaller than the one obtained with the NNPDF2.1 global analysis, but compatible within the PDF uncertainty. The χ^2 per degree of freedom of the $t\bar{t}$ data point to $\sigma_{t\bar{t}}^{\text{th.}}$ is 1.6. After including the $t\bar{t}$ measurement in the fit the predicted cross section moves to $\sigma_{t\bar{t}}^{\text{th.}} = 167.5 \pm 6.8$ (PDF) pb and the χ^2 decreases to 0.4. In Figure 4 we show the change of the gluon PDF and of the gg luminosity due to the new fit. The shift of the central value of the gluon is now significant, and it goes in the same direction as the shift when the jet data is included, bringing the black central line closer to one, which is the reference gluon of the global NNPDF2.1 fit. This can be expected since, as we observed earlier, the χ^2 per degree of freedom to the

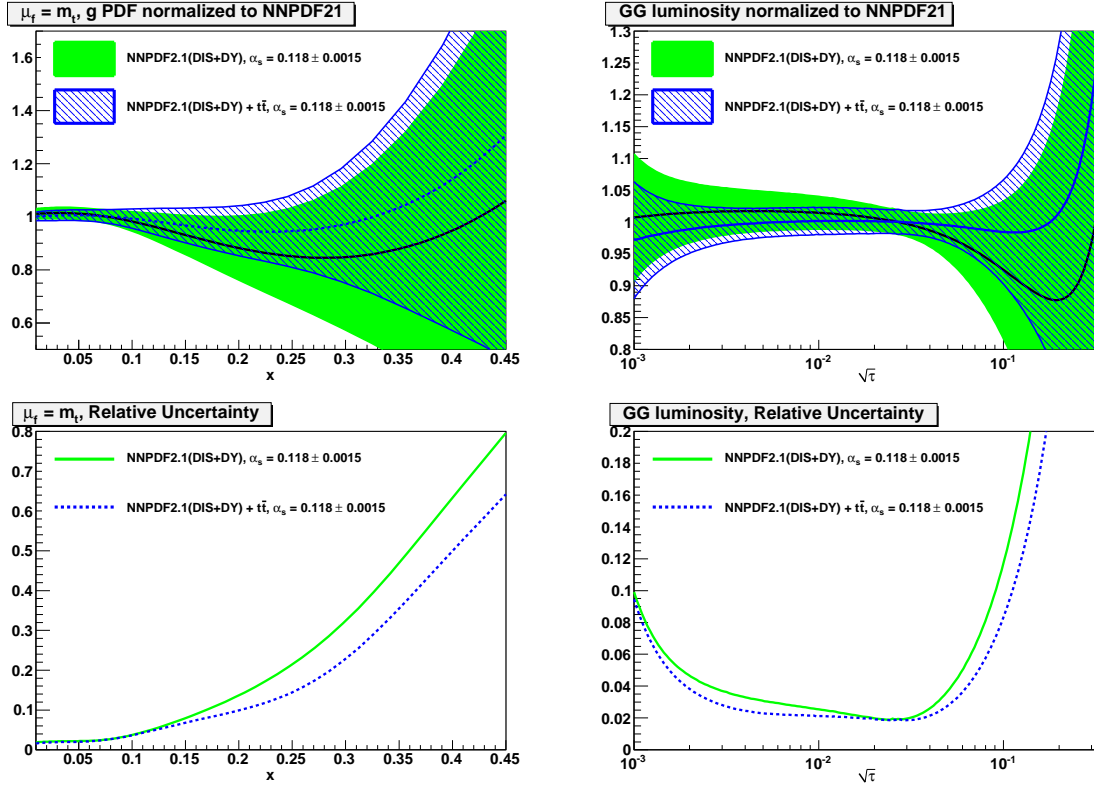


Figure 4: Effect of including the total $t\bar{t}$ cross section measurement (but excluding jet data) on the NNPDF2.1_DIS+DY PDF sets for varying α_s . Top: Gluon distribution (left) and gg luminosity (right) before (solid, solid green in color) and after (shaded, shaded blue in color) the inclusion of the $t\bar{t}$ measurement in the NNPDF fit. Both curves are normalized to the central value of the NNPDF2.1 gluon. Bottom: Half-width of the error bands before (solid, solid green in color) and after (dashed, dashed blue in color) including the $t\bar{t}$ measurement in the fit.

Tevatron jet data in the NNPDF2.1 global fit slightly improved with the inclusion of the $t\bar{t}$ measurement in the fit. A similar observation holds for the gg luminosity. The error reduction is significant and amounts to about 35% both for the gluon at large- x and the gluon-gluon luminosity at medium-large $\sqrt{\tau}$. If we compare the size of the blue error band in Figure 4 to the one of the green error band in Figure 2, we see that the error reduction due to the inclusion of the jet data is certainly larger, by a factor 4, due to the larger number of data included. However, it is striking that the single $t\bar{t}$ data point already has a non-negligible effect with respect to the Tevatron jet data.

In Section 3 we observed that the MSTW2008, NNPDF2.1, and CT10 PDF sets predict comparable values for the top-pair production cross sections at the LHC, while the ABM11 prediction is significantly lower than the others. On the left-hand side of Figure 5 we compare the ABM11 gluon luminosity to the NNPDF2.1_DIS+DY and NNPDF2.1 ones, using the same $\alpha_s(M_Z) = 0.118$ for consistency. In the large- x region the ABM11 gluon lumi-

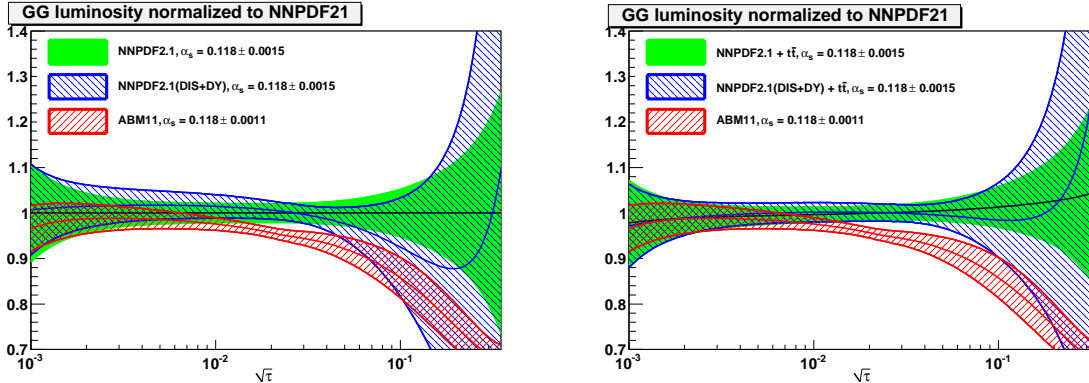


Figure 5: Comparison of gg luminosity obtained in the NNPDF2.1, NNPDF2.1_DIS+DY and ABM11 parton fits before (left) and after (right) the $t\bar{t}$ measurement is included in the NNPDF2.1 and NNPDF2.1_DIS+DY fits. All curves are normalized to the central value of the NNPDF2.1 gluon and computed for $\alpha_s(M_Z) = 0.118$.

osity is about 2σ smaller than NNPDF2.1. It is compatible with NNPDF2.1_DIS+DY, mainly because the uncertainty of the latter is much larger, which in turn is mostly due to differences in the gluon parameterization, and partially also due to a different treatment of the higher-twist effects in DIS.

On the right-hand side of Figure 5 we show the same results but after including the top-pair production cross section in the two NNPDF2.1 fits. We already noted that this increases the large- x gluon and therefore the medium-large $\sqrt{\tau}$ gluon luminosity. A similar effect is expected on the ABM11 gluon and should bring it closer to the other global determinations. But, due to the small uncertainty of the ABM11 gluon, the effect would be much more significant, and the inclusion of the $t\bar{t}$ data might even require a more flexible large- x gluon parameterization.

A caveat to the analysis in the present section must be mentioned, namely that it was performed for a fixed top-quark mass value of $m_t = 173.3$ GeV. A change of ± 1 GeV in the value of m_t , which corresponds to the present top-mass uncertainty, changes the predicted inclusive top production cross section by roughly $\pm 3\%$, which decreases the significance of this measurement for the NNPDF2.1 fit. On the other hand, the difference between the predicted $t\bar{t}$ cross section obtained with the NNPDF2.1 set, $\sigma_{t\bar{t}}^{\text{th.}} = 166.1 \pm 7.3$ (PDF) pb, and with the ABM11 set, $\sigma_{t\bar{t}}^{\text{th.}} = 148.2 \pm 5.9$ (PDF) pb is about 10%, see Table 6. Hence, our conclusion that the present $t\bar{t}$ cross section measurement should already have an impact on the ABM11 fit remains valid after including the top-quark mass uncertainty.

6 Conclusion

In this paper we extended our analysis of the resummed total top-quark pair production cross section [1] in several directions. We updated our results for Tevatron, and for LHC

with 7 and 8 TeV centre-of-mass energy to account for the full $q\bar{q}$ NNLO partonic cross section [9]; studied the dependence on different parton-distribution inputs and the impact of the LHC cross section measurement on the gluon distribution; and presented predictions for heavy “top” quarks. All results and many variations can be obtained with the publicly available program TOPIX, which includes soft and Coulomb resummation. The main results of the present analysis can be summarized as follows:

- Including the full $q\bar{q}$ NNLO partonic cross section removes the slight tension that existed in the prediction of the $t\bar{t}$ cross section at the Tevatron from different groups in favour of the somewhat larger values and reduces the uncertainty by almost a factor of two to about 3%, see also [9]. Our NNLO+NNLL Tevatron $t\bar{t}$ production cross section result, assuming $m_t = 173.3$ GeV and $\alpha_s(M_Z) = 0.1171$, is

$$\sigma_{t\bar{t}} = 7.15_{-0.20}^{+0.21} (\text{theory})_{-0.25}^{+0.30} (\text{PDF}+\alpha_s) \text{ pb} \quad (\text{MSTW2008NNLO}). \quad (6.1)$$

The cross section increases to 7.26 pb, when the “world average” value $\alpha_s(M_Z) = 0.1180$ is used. A top mass $m_t = 171.4_{-5.7}^{+5.4}$ GeV is obtained from Tevatron data.

- Our prediction for the $t\bar{t}$ production cross section at the LHC with $\sqrt{s} = 8$ TeV, assuming $m_t = 173.3$ GeV and $\alpha_s(M_Z) = 0.1171$, is

$$\sigma_{t\bar{t}} = 231.8_{-9.9}^{+9.6} (\text{theory})_{-9.1}^{+9.8} (\text{PDF}+\alpha_s) \text{ pb} \quad (\text{MSTW2008NNLO}). \quad (6.2)$$

The cross section increases to 236.5 pb, when the “world average” value $\alpha_s(M_Z) = 0.1180$ is used.

- The 2011 LHC data from the $\sqrt{s} = 7$ TeV run decrease the uncertainty of the gluon distribution at $x \gtrsim 0.15$ by about 20%, using NNPDF2.1 as the reference gluon. This effect is quite remarkable, given that only a single data point is added to the fit. The precision of the data and theoretical prediction will soon raise the issue of defining a procedure for including consistently theoretical uncertainties into the PDF fits and their error estimates.
- PDF fits including the jet data from the Tevatron agree very well in their predicted top cross section at the LHC. The PDF uncertainty is now the dominant theoretical uncertainty. The ABM11 fit predicts a 10% lower cross section due to its smaller large- x gluon distribution. Our study leads us to expect that the $t\bar{t}$ cross section should already have a significant impact on this fit, even when all theoretical uncertainties, including the top-quark mass input are accounted for.

Acknowledgements

We would like to thank M. Czakon for discussions. The work of M.B., J.P. and M.U. is supported by the DFG Sonderforschungsbereich/Transregio 9 “Computergestützte Theoretische Teilchenphysik”. P.F. acknowledges support by the “Stichting voor Fundamenteel Onderzoek der Materie (FOM)”. This research was supported in part by the National Science Foundation under Grant No. PHY05-51164.

Appendix: Functionality of TOPIXS

In this section we describe the main functionality of the program TOPIXS. A detailed manual is available together with the program package at the URL

<http://users.ph.tum.de/t31software/topixs/>

TOPIXS uses HPLOG [47] for the numerical evaluation of harmonic polylogarithms and QUADPACK [48] for numerical integrations. The PDF sets are included via the LHAPDF [49] library. The determination of the auxiliary parameter β_{cut} and the fixed soft scale, which are used in the computation of the resummed cross section, uses routines from the GNU Scientific Library [50].

The program package consists of several FORTRAN and C++ programs which implement the calculation of the total cross section as well as that of the parameter β_{cut} and the fixed soft scale. The user interface consists of a BASH shell script, called `topixs`, which automatically compiles and executes these programs. The user can change the program settings by editing a single text file. Examples of such a configuration file are included in the program package.

In our approach the cross section depends either on the auxiliary parameter β_{cut} or the fixed soft scale. While programs for their computation are provided, we have also implemented default values for several PDF sets as well as the values for heavy quarks discussed in Section 4. Therefore, it is usually not necessary to compute them, in which case the GNU Scientific Library is not required either.

Several approximations can be chosen for the cross-section computation. A fixed-order calculation is possible to NLO or NNLO_(app) accuracy. In the latter case, the user can choose whether or not to include the full result for the $q\bar{q}$ channel by changing the value of the variable `QQNNLOEXACT` in the configuration file. The resummed cross section can be evaluated in all of the different approximations defined in [1], i.e. (N)NLL₁ and (N)NLL₂ with fixed soft scale, and (N)NLL₂ with running soft scale. The option `BOUNDS` allows the user to decide whether or not to include the contribution from bound states, or even to compute only this contribution.

Our default choice is to use a running soft scale (`MUSRUN=1`) and include the bound-state contribution (`BOUNDS=1`). The full result for the $q\bar{q}$ channel is included in the NNLO computation and the matching of NNLL₂ (`QQNNLOEXACT=1`). These settings will be used unless the variables are explicitly reset in the configuration file.

The main parameters of the calculation are the top-quark mass, the collider type (proton-proton or proton-antiproton) and energy, and the PDF set to be used. All of them can be chosen by the user. The default settings are $m_t = 173.3$ GeV (`MTOP=173.3`), LHC with $\sqrt{s} = 8$ TeV (`COLLIDER=1` and `SQRTS=8000`), and MSTW2008 (`PDFSET=MSTW08`). There are four additional predefined PDF sets: ABM11, NNPDF2.1, JR09 [40], and CT10. For these sets the computation of the PDF+ α_s error is completely automated and it is possible to vary the value of $\alpha_s(M_Z)$ (except for JR09 where no fits with different values of $\alpha_s(M_Z)$ are provided). Other sets can be used by specifying the grid file name. It is also possible to choose a particular member of a PDF set to be used in the calculation. This

can be used to vary α_s with a user specified grid file or for a re-weighting computation as in Section 5.

The theory error is determined by the variation of the various scales (hard, soft, factorization, resummation, and Coulomb) and other parameters like β_{cut} (cf. [1] for a detailed explanation). The central values of these scales can be chosen by the user. The variation is done automatically by evaluating the cross section at several equidistant points between twice and half the central value. The number of points can also be chosen by the user. Alternatively, the user can vary the scales by hand by performing the calculation without error computation (`NOERR=1`) for different values of the scales. This also makes it possible to evaluate the cross section for specifically chosen points.

The computation time strongly depends on the choice of the PDF set, with ABM11 being the fastest and NNPDF2.1 the slowest (this was also noted in [11]). On an AMD Phenom 9850 processor with 2.5 GHz, the computation of a single cross section point (without any error estimates, using the default settings) takes approximately 15 seconds for ABM11, 75 seconds for MSTW2008, and 6 minutes for NNPDF2.1. Using the default configuration file to perform the computation of the NNLO_{app} and NNLL₂ approximations with MSTW2008, including the full theory and PDF+ α_s error, requires the evaluation of several hundreds of cross section points and takes about ten hours.

References

- [1] M. Beneke, P. Falgari, S. Klein, and C. Schwinn, *Nucl.Phys.* **B855** (2012) 695–741, [arXiv:1109.1536 \[hep-ph\]](#).
- [2] M. Beneke, M. Czakon, P. Falgari, A. Mitov, and C. Schwinn, *Phys. Lett.* **B690** (2010) 483–490, [arXiv:0911.5166 \[hep-ph\]](#).
- [3] M. Aliev *et al.*, *Comput. Phys. Commun.* **182** (2011) 1034–1046, [arXiv:1007.1327 \[hep-ph\]](#).
- [4] M. Cacciari, M. Czakon, M. L. Mangano, A. Mitov, and P. Nason, *Phys.Lett.* **B710** (2012) 612–622, [arXiv:1111.5869 \[hep-ph\]](#).
- [5] M. Czakon and A. Mitov, [arXiv:1112.5675 \[hep-ph\]](#).
- [6] V. Ahrens, A. Ferroglia, M. Neubert, B. D. Pecjak, and L. L. Yang, *Phys.Lett.* **B703** (2011) 135–141, [arXiv:1105.5824 \[hep-ph\]](#).
- [7] N. Kidonakis, *Phys. Rev.* **D82** (2010) 114030, [arXiv:1009.4935](#).
- [8] S. J. Brodsky and X.-G. Wu, *Phys. Rev.* **D86** (2012) 014021, [arXiv:1204.1405 \[hep-ph\]](#).
- [9] P. Bärnreuther, M. Czakon, and A. Mitov, [arXiv:1204.5201 \[hep-ph\]](#).

- [10] A. D. Martin, W. J. Stirling, R. S. Thorne, and G. Watt, *Eur. Phys. J.* **C63** (2009) 189–285, arXiv:0901.0002 [hep-ph].
- [11] S. Alekhin, J. Blümlein, and S. Moch, arXiv:1202.2281 [hep-ph].
- [12] P. M. Nadolsky, H.-L. Lai, Q.-H. Cao, J. Huston, J. Pumplin, *et al.*, *Phys.Rev.* **D78** (2008) 013004, arXiv:0802.0007 [hep-ph].
- [13] G. Watt, *JHEP* **1109** (2011) 069, arXiv:1106.5788 [hep-ph].
- [14] The NNPDF Collaboration, R. D. Ball *et al.*, *Nucl.Phys.* **B849** (2011) 112–143, arXiv:1012.0836 [hep-ph].
- [15] R. D. Ball, V. Bertone, F. Cerutti, L. Del Debbio, S. Forte, *et al.*, *Nucl.Phys.* **B855** (2012) 608–638, arXiv:1108.1758 [hep-ph].
- [16] M. Beneke, P. Falgari, and C. Schwinn, *Nucl. Phys.* **B828** (2010) 69–101, arXiv:0907.1443 [hep-ph].
- [17] M. Beneke, P. Falgari, and C. Schwinn, *Nucl. Phys.* **B842** (2011) , arXiv:1007.5414 [hep-ph].
- [18] T. Becher and M. Neubert, *Phys. Rev. Lett.* **97** (2006) 082001, hep-ph/0605050.
- [19] T. Becher, M. Neubert, and G. Xu, *JHEP* **07** (2008) 030, arXiv:0710.0680 [hep-ph].
- [20] U. Langenfeld, S. Moch, and P. Uwer, *Phys. Rev.* **D80** (2009) 054009, arXiv:0906.5273 [hep-ph].
- [21] A. D. Martin, W. J. Stirling, R. S. Thorne, and G. Watt, *Eur. Phys. J.* **C64** (2009) 653–680, arXiv:0905.3531 [hep-ph].
- [22] M. Beneke, P. Falgari, S. Klein, and C. Schwinn, arXiv:1112.4606 [hep-ph], in: *Proceedings of the 10th International Symposium on Radiative Corrections (RADCOR2011)*.
- [23] D0 Collaboration, V. M. Abazov *et al.*, *Phys.Lett.* **B703** (2011) 422–427, arXiv:1104.2887 [hep-ex].
- [24] D0 Collaboration, V. M. Abazov *et al.*, *Phys.Lett.* **B704** (2011) 403–410, arXiv:1105.5384 [hep-ex].
- [25] Tevatron Electroweak Working Group, CDF and D0 Collaborations, arXiv:1107.5255 [hep-ex].
- [26] ATLAS Collaboration, *Measurement of the $t\bar{t}$ production cross-section in pp collisions at $\sqrt{s} = 7$ tev using kinematic information of lepton+jets events*, Tech. Rep. ATLAS-CONF-2011-121, CERN, Geneva, Aug, 2011.

- [27] CMS Collaboration, M. Aldaya, K. Lipka, and S. Naumann-Emme, [arXiv:1201.5336](#) [hep-ex].
- [28] M. Beneke, P. Falgari, S. Klein, J. Piclum, and C. Schwinn, [arXiv:1205.0988](#) [hep-ph]. *Proceedings of the 47th Rencontres de Moriond on QCD and High Energy Interactions, March 10-17, 2012, La Thuile, Italy.*
- [29] S. Moch, P. Uwer, and A. Vogt, *Phys.Lett.* **B714** (2012) 48–54, [arXiv:1203.6282](#) [hep-ph].
- [30] A. Ferroglia, B. D. Pecjak, and L. L. Yang, [arXiv:1205.3662](#) [hep-ph].
- [31] R. D. Ball, V. Bertone, F. Cerutti, L. Del Debbio, S. Forte, *et al.*, *Nucl.Phys.* **B849** (2011) 296–363, [arXiv:1101.1300](#) [hep-ph].
- [32] H.-L. Lai, M. Guzzi, J. Huston, Z. Li, P. M. Nadolsky, *et al.*, *Phys.Rev.* **D82** (2010) 074024, [arXiv:1007.2241](#) [hep-ph].
- [33] H.-L. Lai, J. Huston, Z. Li, P. Nadolsky, J. Pumplin, *et al.*, *Phys.Rev.* **D82** (2010) 054021, [arXiv:1004.4624](#) [hep-ph].
- [34] N. Arkani-Hamed, A. Cohen, E. Katz, and A. Nelson, *JHEP* **0207** (2002) 034, [arXiv:hep-ph/0206021](#) [hep-ph].
- [35] M. Perelstein, M. E. Peskin, and A. Pierce, *Phys.Rev.* **D69** (2004) 075002, [arXiv:hep-ph/0310039](#) [hep-ph].
- [36] K. Agashe, R. Contino, L. Da Rold, and A. Pomarol, *Phys.Lett.* **B641** (2006) 62–66, [arXiv:hep-ph/0605341](#) [hep-ph].
- [37] CMS Collaboration, S. Chatrchyan *et al.*, *JHEP* (2012) , [arXiv:1204.1088](#) [hep-ex].
- [38] CMS Collaboration, S. Chatrchyan *et al.*, [arXiv:1203.5410](#) [hep-ex].
- [39] CMS Collaboration, S. Chatrchyan *et al.*, *Phys.Rev.Lett.* **107** (2011) 271802, [arXiv:1109.4985](#) [hep-ex].
- [40] P. Jimenez-Delgado and E. Reya, *Phys.Rev.* **D80** (2009) 114011, [arXiv:0909.1711](#) [hep-ph].
- [41] H1 and ZEUS Collaboration, F. Aaron *et al.*, *JHEP* **1001** (2010) 109, [arXiv:0911.0884](#) [hep-ex].
- [42] G. Watt and R. Thorne, [arXiv:1205.4024](#) [hep-ph].
- [43] ATLAS Collaboration, G. Aad *et al.*, *JHEP* **1205** (2012) 059, [arXiv:1202.4892](#) [hep-ex].

- [44] ATLAS Collaboration, *Measurement of $t\bar{t}$ production in the all-hadronic channel in 1.02 fb^{-1} of pp collisions at $\sqrt{s} = 7 \text{ TeV}$ with the ATLAS detector*, Tech. Rep. ATLAS-CONF-2011-140, CERN, Geneva, Sep, 2011.
- [45] CMS Collaboration, *Combination of top pair production cross section measurements*, Tech. Rep. CMS-PAS-TOP-11-024, CERN, Geneva, 2011.
- [46] J. M. Campbell, J. Huston, and W. Stirling, *Rept.Prog.Phys.* **70** (2007) 89, [arXiv:hep-ph/0611148](#) [hep-ph].
- [47] T. Gehrmann and E. Remiddi, *Comput.Phys.Commun.* **141** (2001) 296–312, [arXiv:hep-ph/0107173](#) [hep-ph].
- [48] R. Piessens, E. de Doncker-Kapenga, C. Überhuber, and D. Kahaner, *QUADPACK: A Subroutine Package for Automatic Integration*. Springer Series in Computational Mathematics. Springer Verlag, 1983.
- [49] M. Whalley, D. Bourilkov, and R. Group, [arXiv:hep-ph/0508110](#) [hep-ph].
- [50] M. Galassi *et al.*, *GNU Scientific Library Reference Manual*. Network Theory Ltd., 3rd ed., 2009.